Published in final edited form as:
Cell Metab. 2012 February 8; 15(2): 171–185. doi:10.1016/j.cmet.2012.01.004.

Altered Mitochondrial Function and Metabolic Inflexibility Associated with Loss of Caveolin-1

Ingrid Wernstedt Asterholm[1], **Dorothy I. Mundy**[1,2], **Jian Weng**[2], **Richard G. W. Anderson**[2,‡], and **Philipp E. Scherer**[1,2]

[1]Touchstone Diabetes Center, Departments of Internal Medicine University of Texas Southwestern Medical Center, Dallas, TX

[2]Cell Biology, University of Texas Southwestern Medical Center, Dallas, TX

Abstract

Caveolin-1 is a major structural component of raft structures within the plasma membrane and has been implicated as a regulator of cellular signal transduction with prominent expression in adipocytes. Here, we embarked on a comprehensive characterization of the metabolic pathways dysregulated in caveolin-1 null mice. We found that these mice display decreased circulating levels of total and high molecular weight adiponectin and a reduced ability to change substrate use in response to feeding/fasting conditions. Caveolin-1 null mice are extremely lean, but retain muscle mass despite lipodystrophy and massive metabolic dysfunction. Hepatic gluconeogenesis is chronically elevated, while hepatic steatosis is reduced. Our data suggest that the complex phenotype of the caveolin-1 null mouse is caused by altered metabolic and mitochondrial function in adipose tissue with a subsequent compensatory response driven mostly by the liver. This mouse model highlights the central contributions of adipose tissue for system-wide preservation of metabolic flexibility.

Introduction

Caveolin-1 is an important structural component of caveolae, omega-shaped lipid rafts rich in cholesterol and sphingolipids (Drab et al., 2001). These plasma membrane compartments facilitate the interaction of receptors with downstream effectors and are found in many different cell types, but most prominently in endothelial cells as well as in adipocytes where caveolae can make up to 20–30% of total plasma membrane area (Fan et al., 1983). In addition to signaling, caveolin-1 also plays an important role in intracellular cholesterol and sphingolipid transport (Liu et al., 2002; Sonnino and Prinetti, 2009).

Mice lacking caveolin-1 display a variety of phenotypes. While the mice are phenotypically nearly normal in the unchallenged state, they have an increased propensity for malignant

Correspondence to: Philipp E. Scherer, the Touchstone Diabetes Center, Department of Internal Medicine, University of Texas Southwestern Medical Center, 5323 Harry Hines Blvd., Dallas, TX, 75390-8549. Philipp.Scherer@utsouthwestern.edu Tel: 214-648-8715; Fax: 214-648-8720.

‡This paper is dedicated to the memory of our wonderful colleague, Dr. Richard Anderson, who recently passed away.

Supplemental Information Supplemental Information includes Supplemental Experimental Procedures, six Figures, and one additional Table appear with this article online at.....

transformation (Williams and Lisanti, 2005). Metabolically, earlier studies show that they have reduced whole body fat mass, elevated triglyceride levels, elevated postprandial free fatty acid (FFA) levels, lower adiponectin levels and a blunted response to β3-adrenergic receptor (β3-AR) stimulation (Cohen et al., 2004; Razani et al., 2002). Moreover, Cohen et al demonstrate that caveolin-1 is necessary for appropriate insulin signaling selectively in adipose tissue, but not in muscle or liver (Cohen et al., 2003). However, a more detailed metabolic characterization has not yet been performed on these mice.

Our past work focused on metabolic flexibility of adipose tissue. Metabolic flexibility refers to the ability of adipocytes to rapidly adapt to changes in metabolic state and to activate compensatory cellular pathways enabling them to appropriately buffer excess influx and consumption of calories, thereby maintaining systemic energy homeostasis. This functional definition of metabolic flexibility is overlapping with the description that other groups in the field have used (Sparks et al., 2009). We have recently shown that mice with a transgene-mediated overproduction of adiponectin display enhanced metabolic flexibility. These mice exhibit increased sensitivity to β3-AR-agonists and increased mitochondrial function (Asterholm and Scherer, 2010). In many ways, mice lacking caveolin-1 display the opposite phenotype, including a decreased sensitivity to β3-AR-agonists. Here, we aim to carefully dissect the individual components that lead to the metabolic phenotype of caveolin-1 null mice. We found that caveolin-1 deficiency leads to substantial metabolic alterations, including a prominent metabolic inflexibility and an increase in hepatic glucose production. Our data highlight that metabolic dysregulation at the level of adipose tissue is the major driving force for the complex systemic changes observed in caveolin-1 null mice.

Results

Caveolin-1 null mice have lower plasma adiponectin levels

We have previously observed that mice overexpressing adiponectin displayed elevated caveolin-1 levels in adipocytes (Combs et al., 2004). Furthermore, an initial phenotypic characterization of the caveolin-1 null mouse showed some degree of metabolic impairment, even though the underlying mechanistic reasons were not understood at the time (Cohen et al., 2004; Cohen et al., 2003; Razani et al., 2002). Our recent work on the adipocyte-derived secretory protein adiponectin indicated that mice over-expressing adiponectin showed increased “metabolic flexibility”, i.e. an ability to adjust effectively to changing total nutrient availability and/or lipid or carbohydrate as primary fuel source (Asterholm and Scherer, 2010). We therefore tested whether the metabolic phenotype of caveolin-1 null mice could be explained through a reduction of adiponectin levels. We assessed adiponectin expression at both mRNA and the intracellular protein level as well as at the total circulating adiponectin level and the different adiponectin isoforms. Adiponectin mRNA levels were increased, while intracellular adiponectin protein levels were unaltered in adipose tissue. However, total adiponectin levels in circulation as well as the relative proportion of the HMW form were significantly reduced in the caveolin-1 null mice (Fig. 1A–C). The difference in isoform distribution was independent of the differences in total levels as the variability in adiponectin levels within genotypes made it possible to match a subset of the wildtype and caveolin-1 null samples for equal total levels. Consistent with previous observations (Cohen et al., 2004), caveolin-1 null mice were essentially unresponsive to β3-AR agonist stimulation as judged by impaired β3-AR agonist-induced release of FFAs (Fig. 1D). This was also associated with impaired β3-AR agonist-mediated insulin release, an effect directly linked to effects in the adipocyte (Grujic et al., 1997) (Fig. 1E). Caveolin-1 null mice also displayed a significantly reduced fat mass as previously reported (data not shown) (Razani et al., 2002).

Reduced “metabolic flexibility“ in caveolin-1 null mice

We have previously shown that decreased adiponectin levels are associated with reduced metabolic flexibility as judged by the inability to properly respond to β3-AR agonist and overall reduced insulin sensitivity (Asterholm and Scherer, 2010). We wanted to test whether this reduces the ability of the mouse to adapt to other metabolic challenges, such as physiological fast. Fasting is known to induce hepatic steatosis secondary to the increased levels of circulating FFAs released through lipolysis in adipose tissue. We assessed hepatic steatosis before and after a 24h fast by computerized tomography (Asterholm and Scherer, 2010). Wildtype mice displayed the expected increase in hepatic lipid accumulation, while this response was significantly blunted in the caveolin-1 null mice (Fig. 2A–B). An alternative test to probe metabolic flexibility is the response to an alternate day fasting (ADF) regimen. The alternation of one day of fasting followed by one day of *ad libitum* access to food has previously been shown to remodel adipose tissue, and in fact improves whole body metabolism in mice (Varady et al., 2009; Varady and Hellerstein, 2007). Wildtype control mice and caveolin-1 null mice were first fed a high fat diet (HFD) for 8 weeks, followed by either ADF or continued *ad libitum* feeding for an additional 4 weeks. Consistent with previous studies, the caveolin-1 null mice were protected against HFD-induced obesity (data not shown and (Razani et al., 2002)). The reduced weight gain was also associated with reduced hepatic steatosis after HFD exposure (Fig. 2C). This observation is in sharp contrast to other lipodystrophic mouse models in which the inability to store fat causes increased ectopic lipid storage in the liver (Asterholm et al., 2007). Wildtype mice benefitted from the ADF regimen with respect to hepatic steatosis, while there was no impact in the caveolin-1 null mice (Fig. 2D). This is not solely due to the lower baseline lipid level in the caveolin-1 null mice after HFD, since a clear increase in hepatic lipid content in caveolin-1 null mice after HFD exposure is apparent as well (Fig. 2C). Body weights within the genotypes were similar between ADF and the *ad libitum* fed mice (WT: 37.8 +/− 1.4 vs 39.1 +/− 1.6, p=0.6 and Cav1−/−: 33.9 +/− 0.8 vs 30.8 +/− 1.3, p=0.13 for ad lib vs. ADF). Liver weights in relation to body weights were increased in caveolin-1 null mice under all conditions (chow diet, HFD, HFD ADF) (Suppl. Fig. 1A), indicating that the liver may be a key organ that compensates to maintain normal systemic metabolism.

The respiratory exchange ratio (RER) reflects preferences for fuel utilization, with RERs near 0.7 indicating predominant use of FFAs as energy source, whereas RERs around 1.0 reflect preferential use of carbohydrates. The rate at which the RER changes between fasting (preferential FFA use) versus fed (enhanced carbohydrate use) is a reflection of the “metabolic flexibility” of a mouse in terms of adapting to altered fuel availability. We measured the RER calculated from O_2 consumption and CO_2 production data obtained in metabolic cages in chow fed mice. We found that the variability of RER over a 24h period was reduced in the caveolin-1 null mice, i.e. RER remained high also during the light phase (Fig. 2E). This suggests that the caveolin-1 null mice are generally less adept to switching fuel sources and display an increased propensity towards carbohydrate metabolism. We also observed an increase in food intake (Suppl. Fig. 1B) and an increase in O_2 consumption (Suppl. Fig. 1C) in the caveolin-1 null mice. In another set of mice, we measured RER during a 24h fast, a state with the highest possible rates of fatty acid oxidation, and found that RER was higher in the caveolin-1 null mice compared to the wild type controls. This is consistent with a reduced capacity for whole-body fatty acid oxidation in caveolin-1 null mice (Suppl. Fig 1D). Since caveolin-1 null mice display a lower capacity for whole-body fatty acid oxidation and are less adept at storing excess energy in adipose tissue compared to wild type mice, we expected to see an increase in hepatic lipid accumulation. Surprisingly however, rather than seeing an elevation, we observed reduced levels of lipid accumulation (Fig. 2A–B). This prompted us to investigate the response to feeding/fasting in these mice further.

Normal fasting-induced increase in circulating FFAs, but reduced hepatic steatosis in the caveolin-1 null mice

Our data (Fig. 1D,E, and (Cohen et al., 2004; Mattsson et al., 2010)) strongly support that the lipolytic response to β3-AR stimulation is impaired in the caveolin-1 null mice. The direct impact on fasting-induced lipolysis has however not been examined in great detail, even though we expected to see this process impaired as well. Surprisingly, fasting triggered equally high FFA levels in caveolin-1 null mice as in wildtype mice (Fig. 2F), despite reduced levels of phosphorylated hormone-sensitive lipase (HSL) (Suppl. Fig. 1E), with overlapping kinetics. This clearly suggests that under normal physiological conditions, caveolin-1 null mice do not display impaired mobilization of FFAs (Fig. 2F) and have elevated triglyceride levels (Suppl. Fig 1F). A similar phenomenon is seen in β1/2/3-AR knock out mice that also have normal lipolysis during a physiological fast (Jimenez et al., 2002). Hence, the preferential use of carbohydrates in caveolin-1 null mice and the reduced hepatic steatosis is not a function of limited FFA availability. In fact, the caveolin-1 null mice reached even higher glycerol levels than the controls in the fasting state (Fig. 2G), suggesting either increased lipolysis in adipose tissue or a decreased systemic use of glycerol.

In the fed state, insulin levels were higher in caveolin-1 null mice, while glucose levels were comparable, and hepatic glycogen levels were reduced (16.9 +/− 4.8 vs. 5.2 +/− 0.7 mg/g, $p<0.05$), indicative of a prevailing degree of insulin resistance in this system (Fig. 3A–B). In the fasted state, the caveolin-1 null mice maintained their glucose levels better than wildtype mice, suggesting enhanced glucose production. In further support for the enhanced hepatic gluconeogenic potential, we found increased glycogen levels in the livers of moderately fasted caveolin-1 null mice (Fig. 3C). Upon re-feeding, the caveolin-1 null mice displayed fairly severe hyperglycemia and a delayed suppression of FFA levels, further reflecting insulin resistance and a poor adaption to altered metabolic conditions and (Fig. 2F and 3B). During a fast, the caveolin-1 null mice lost considerably more body weight than wildtype mice (Fig. 3D). CT analysis showed that the increased weight loss was caused equally much by loss of fat and lean body mass (wildtype to caveolin-1 null mice: fat loss ≈0.6 vs. 0.9 g, $p=0.18$, lean body mass loss wildtype to caveolin-1 null mice: ≈1.7 vs. 2.0 g, $p=0.11$).

Enhanced hepatic gluconeogenesis in the caveolin-1 null mouse

To further understand the underlying mechanism for the enhanced glucose production, we compared the gene expression pattern in livers from 5h fasted wildtype and caveolin-1 null mice. Amongst the genes implicated in gluconeogenesis, glucose-6-phosphatase and lactate dehydrogenase were transcriptionally significantly up-regulated in the caveolin-1 null mice (Suppl. Table 1). More strikingly, components of the urea cycle were among the most up-regulated genes in the caveolin-1 null mice (Suppl. Table 1). This may be a reflection of increased catabolism of amino acids in caveolin-1 null livers. Consistent with the hepatic gene expression profile, plasma urea levels were also elevated in caveolin-1 null mice (Fig. 3E) despite any signs of muscle wasting in these animals (Mattsson et al., 2010; Razani et al., 2002). The skeletal muscle tissue of caveolin-1 null mice also has a much darker appearance (Suppl. Fig. 2A), indicative of myotubes with increased mitochondrial content. There was an overall downregulation of the mitochondrial transcriptional program (Suppl. Table 1). On the other hand, carnitine/acylcarnitine translocase was upregulated, an indication of an increased flux of fatty acylcarnitines and possibly an increased rate of incomplete fatty acid oxidation leading to elevated levels of acetyl-CoA in the liver. In addition, a number of genes involved in peroxisomal β-oxidation were upregulated in the caveolin-1 null mice (Suppl. Table 1). Peroxisomes are thought to mainly catabolize branched-chain fatty acids and very long-chained fatty acids, i.e. lipid species that cannot be efficiently transported into the mitochondrial matrix as they are poor substrates for Cpt1.

However, peroxisomal fatty acid oxidation does not generate ATP. Instead, each cycle of oxidation results in a shorter fatty acid, acetyl-CoA and H_2O_2. Accumulation of acetyl-CoA is the main trigger for the activation of pyruvate carboxylase, which in turn is an established positive regulator of gluconeogenesis. In line with the transcriptional changes, acetyl-carnitine levels, which are a good reflection of the levels of acetyl-CoA (Carlin et al., 1990) do indeed accumulate in the liver of caveolin-1 null mice (Fig. 3F).

An important rate-limiting step for the rate of gluconeogenesis is the enzyme fructose-1,6-bisphosphatase whose activity is dependent on its phosphorylation state regulated by a cAMP-dependent kinase (el-Maghrabi et al., 1982). We therefore tested the effects of a phospodiesterase inhibitor (enoximone) on glucose levels. Enoximone very potently increases glucose levels in caveolin-1 null mice, while the same dose had no effect in the wildtype controls (Fig. 3G). Enoximone also had no effect on glycerol, FFA and H_2O_2 levels in wildtype mice, while caveolin-1 mice displayed increased glycerol, reduced FFA levels and increased H_2O_2 levels (Fig. 3H and data not shown). These dramatic physiological differences are likely due to the availability of very high levels of gluconeogenic substrates that allow these mice to mount a massive gluconeogenic response the moment the animals face an increase in hepatic cAMP levels. The increased glycerol levels indicate a concomitant enhancement of lipolysis, a reflection of the enhanced sensitivity to cAMP in adipose tissue. This in turn is linked to the reduced sensitivity to adrenergic stimulation at the level of agonist-receptor interaction. In parallel, the excess FFAs that are generated under these conditions are likely to be metabolized and used as fuel for gluconeogenesis.

Hepatic fatty acid oxidation and gluconeogenesis are processes that are tightly connected. Increased fatty acid oxidation (e.g. by stimulation with PPARα agonists) has been to shown to enhance gluconeogenesis, while liver-specific PEPCK−/− mice get enhanced hepatic steatosis due to a reduction in fatty acid oxidation (Burgess et al., 2004; Oosterveer et al., 2009). Thus, changes in gluconeogenesis affect fatty acid oxidation and *vice versa*. Therefore, we hypothesized that the increased glucose production in the caveolin-1 null mice is associated with an increase in hepatic fatty oxidation that would explain the reduced fasting-induced steatosis. In a first set of studies, we gave 3-mercaptopicolinic acid (3-MPA), a specific PEPCK-inhibitor (Goodman, 1975), to 5h fasted wildtype and caveolin-1 null mice. 3-MPA exposure caused a more dramatic drop in glucose levels in caveolin-1 null mice compared to wildtype mice, indicating that PEPCK-dependent gluconeogenesis plays an important role in maintaining normal glucose levels in moderately fasted caveolin-1 null mice (Fig. 4A). As expected, in wildtype mice, there was a small but continuous decrease in glucose levels throughout the 3h time course. In contrast, the glucose levels in the caveolin-1 null mice returned to baseline levels towards the end of the time course. To obtain more insights into the substrate flux in the caveolin-1 null mice, we followed the circulating levels of insulin, glucagon, lactate, glycerol and FFAs over the same period. Insulin and glucagon levels were similar in between wild type and caveolin-1 null mice throughout the time course (data not shown). Lactate and glycerol levels were similar in wildtype and caveolin-1 null mice at baseline. However, upon 3-MPA treatment, the levels of both lactate and glycerol increased in the caveolin-1 null mice, while the levels generally decreased in the wildtype mice (Fig. 4B–C). The increased lactate levels in the caveolin-1 null mice indicate a preference for aerobic glycolysis as opposed to oxidative phosphorylation. Thus, the normal baseline lactate levels in caveolin-1 null mice may be a reflection of increased production as well as increased use of lactate for gluconeogenesis in the liver. Alternatively, the elevated lactate levels reflect a reduced uptake and utilization of lactate in the context of PEPCK-inhibition in the caveolin-1 nulls. The increase in the glycerol levels in the caveolin-1 null mice suggests either increased lipolysis and/or reduced use of glycerol for (PEPCK-independent) gluconeogenesis. FFA levels remained fairly

constant and followed the glycerol levels in the wildtype mice. In the caveolin-1 null mice however, 3-MPA causes an immediate drop in FFA levels followed by a slower recovery (data not shown), indicating an increased use of these FFAs (outside the liver) in response to the reduction in glucose. Indeed, we observed an acylcarnitine fingerprint which is indicative of an enhanced fatty acid oxidation in skeletal muscle that may explain the reduction in FFA during both the 3-MPA and the enoximone experiments (Adams et al., 2009) (Suppl. Fig. 2B). The reduction in lactate and glycerol levels in wildtype mice follows the anticipated metabolic adaptation to reduced PEPCK-dependent gluconeogenesis, i.e. increased use of glycerol for glucose production as well as reduced glycolysis due to a switch to fatty acid oxidation.

To further explore the fasting response, we followed hepatic steatosis for 24 hours in mice treated intermittently with 3-MPA or vehicle. 3-MPA treatment increased fasting-induced steatosis in caveolin-1 null mice to about the same levels as seen in vehicle-treated wildtype mice. 3-MPA-treated wildtype mice had even more aggravated fasting-induced steatosis (Fig. 4D). These are longitudinal measurements of hepatic lipid accumulation using CT scanning of the liver as described previously (Asterholm and Scherer, 2010). Since the 3-MPA treated mice had increased hepatic triglyceride levels, we conclude that a reduction of PEPCK-mediated gluconeogenesis increases hepatic steatosis through a reduction of hepatic fatty acid oxidation. Chronically 3-MPA treated caveolin-1 null mice still maintained glucose levels better than wildtype mice (Fig. 4E). This suggests that caveolin-1 null mice are rapidly able to overcome the acute hypoglycemic effects of 3-MPA, but this adaptive response is not quite as effective of an “enhancer” of hepatic fatty acid oxidation as the PEPCK-dependent gluconeogenesis is in the absence of 3-MPA.

The first step in PEPCK-dependent gluconeogenesis begins in the mitochondria with the formation of oxaloacetate through carboxylation of pyruvate. This reaction requires one molecule of ATP and is catalyzed by pyruvate carboxylase, an enzyme that is stimulated by high acetyl-CoA levels (Utter et al., 1964). In contrast, glycerol enters the gluconeogenic pathway through phosphorylation to glycerol-3-phosphate by glycerol kinase and dehydrogenation to dihydroxyacetone phosphate by glyceraldehyde-3-phosphate dehydrogenase. This pathway requires less ATP and is not regulated by acetyl-CoA, and may therefore be less tightly coupled to increased fatty acid oxidation as compared to PEPCK-mediated gluconeogenesis. Furthermore, an up-regulation of the gluconeogenic pathway may protect against hepatic steatosis through a reduced availability of glycerol for triglyceride synthesis. To test whether caveolin-1 null mice have an enhanced ability to use glycerol for glucose production, we injected 3-MPA treated mice with a bolus of glycerol. We found that the caveolin-1 null mice indeed had enhanced glycerol-induced glucose production (Fig. 4F). However, glycerol clearance was delayed (Suppl. Fig. 3A). While we see a strong increase in gluconeogenesis, other glycerol consuming pathways, such as triglyceride synthesis through glycerol kinase-induced conversion of glycerol to glycerol-3-phospate, may be reduced in the caveolin-1 null mouse. Alternatively, an increased rate of lipolysis in the caveolin-1 null mice would also explain the phenomenon. To directly address the underlying mechanism for the reduction in hepatic steatosis and the altered body composition in the caveolin-1 null mice, we injected a tritium-labeled triolein lipid emulsion intravenously in mice that have been fasted for 5h. Under these conditions, ^{3}H counts in the aqueous phase of all collected tissues were similar in wild type and caveolin-1 null mice (data not shown). However, we found that the ^{3}H counts in the organic phase of the liver were reduced in the caveolin-1 null mice (Fig. 5A). Thus, the reduction in hepatic steatosis in the caveolin-1 null mice is best explained by a reduced hepatic triglyceride synthesis although we cannot rule out that an increase in fatty acid oxidation plays a role during prolonged fasting as well. Surprisingly, we also found that the ^{3}H count in the organic phase of adipose tissue was increased in the caveolin-1 null mice (Fig. 5A). This indicates an

increase in triglyceride synthesis in adipose tissue and strongly suggests that the reduced fat mass in the caveolin- 1 null mice is primarily due to enhanced lipolysis.

The enhanced hepatic glucose output in the caveolin-1 null mouse is a secondary adaptation

To determine whether any of the reported metabolic changes in the liver are a direct consequence of the lack of low level caveolin-1 expression in hepatocytes, we used a newly generated mouse model carrying a floxed version of the caveolin-1 gene (Suppl. Fig. 3B–C), bred into the background of an albumin promoter-driven CRE mouse. In this configuration, we eliminate functional copies of the caveolin-1 gene exclusively from hepatocytes. The gene is effectively rearranged in hepatocytes, but not in other tissues (Suppl. Fig. 3D). We have assayed these mice for fasting-induced steatosis and glycerol-induced glucose production and noted that these mice behaved similar to wildtype mice (Suppl. Fig. 3E). However, the glycerol levels 30 minutes after administration of 3-MPA were significantly lower in liver specific caveolin-1 nulls as compared to control mice (Suppl. Fig. 3F). Furthermore, over the course of a fasting/refeeding experiment, there was a small but significant reduction in fasted glucose levels in the mice lacking hepatic caveolin-1 (Suppl. Fig. 3G). Thus, despite a dramatic change in hepatic metabolism in the full body knock out mouse, the liver-specific caveolin-1 null shows a slight defect in glucose production associated with a more rapid clearance of glycerol, the opposite phenotype observed in the full body knock out animal. We confirmed the absence of caveolin-1 in the liver by looking at liver lipid droplet associated caveolin-1, using full body knock out animals as controls (Suppl. Fig. 3H).

Based on these findings, we conclude that the elevated glucose seen in the caveolin-1 null mice is not due to the actions of caveolin within the liver, consistent with the very low expression level of caveolin-1 in hepatocytes. Instead we propose that the glucose production is driven by higher substrate availability. Specifically, glycerol as a product of elevated lipolysis seems to play a major role as a substrate of particular importance for the elevated glucose production in the caveolin-1 null mice.

Altered mitochondrial function in caveolin-1 null adipose tissue

We reasoned that both the enhanced gluconeogenesis in the liver and the preservation of skeletal muscle in the whole body caveolin-1 null mouse could to a large extent be secondary adaptations to changes in tissues that are rich in caveolin-1, such as adipose tissue (Scherer et al., 1994). In a first attempt to address this hypothesis, we investigated the gene expression profile of gonadal white adipose tissue in caveolin-1 null *vs.* wildtype control mice. This analysis revealed a striking difference with respect to genes involved in mitochondrial function. Most genes related to mitochondria, including branched-chain amino acid (BCAA) catabolic enzymes, were down-regulated in the caveolin-1 null mice (Table 1). qPCR analysis of nuclear expressed mitochondrial genes in subfractionated fat pads showed that the down-regulation of the mitochondrial program is predominantly seen in adipocytes, but not in the stromal vascular fraction of adipose tissue Table 1 and data not shown). However, the protein levels of a key mitochondrial marker (subunit IV of cytochrome oxidase) were similar in between wild type and caveolin-1 null mice, as judged by COXIV levels per milligram total cellular protein (Suppl. Fig. 4A). We also examined the level of carbonylation in adipose tissue (a reflection of oxidative damage recently established by Bernlohr and colleagues (Frohnert et al., 2011; Grimsrud et al., 2008)) and we noticed elevated levels of oxidative damage (Suppl. Fig. 4B). In line with this finding, several redox-sensitive genes are reduced in the gonadal adipose tissue of caveolin-1 null mice (Suppl. Fig. 4C). This includes glutathione S-transferase A4 (GSTA4), the primary enzyme for lipid aldehyde detoxification, thereby explaining the elevated levels of

carbonylated proteins. Mitochondrial function in adipocytes of GSTA4-null mice is significantly impaired, even in the lean state (Curtis et al., 2010). In further support for a presumed mitochondrial change, we observed that caveolin-1 null mice had significantly increased circulating peroxide levels (H_2O_2) in both males and females (Fig. 5B). Concomitant with that, we found a small but highly reproducible decrease of circulating pyruvate levels (Fig. 5C). H_2O_2 converts pyruvate to acetate (Babich et al., 2009). Hence, the reduced levels of pyruvate may be a secondary consequence to the increased presence of H_2O_2. In addition, we also found a strong positive correlation between circulating pyruvate and adiponectin levels in fasted mice across both genotypes in wildtype and caveolin-1 null mice (Fig. 5D). This provides a mechanistic insight for the lowered adiponectin levels in the caveolin-1 null mice and that are linked to the profound metabolic changes seen in the caveolin-1 nulls. Increased ROS levels and mitochondrial dysfunction in adipocytes have been shown to reduce adiponectin levels by interfering with the export of adiponectin through the secretory pathway (Koh et al., 2007). We suggest that an increased pyruvate level is an indicator of reduced ROS production and/or increased endogenous anti-oxidative capacity, which has a positive impact on adiponectin levels. While a causal relationship between these two parameters in the context of oxidative stress remains to be demonstrated, the strong correlations seen between pyruvate and adiponectin hint at a potentially important physiological connection prominently displayed in the caveolin-1 null mouse, but also seen in wildtype mice. Finally, circulating H_2O_2 levels and circulating adiponectin levels show a strong negative correlation (Suppl. Fig. 4D), further establishing a tight link between the local oxidative damage in adipose tissue and systemic metabolic adaptions.

Our *in vivo* characterization of the metabolic phenotype of the caveolin-1 null mice indicates elevated lipolysis as a driving force for the lean phenotype. Direct measurements of FFAs in adipose tissue indeed reveal an approximately two-fold elevation of FFAs in caveolin-1 null adipose tissue as compared to wild type adipose tissue (Fig. 5E). This finding is further supported by an increased infiltration of macrophages, a phenomenon strongly associated with elevated FFAs (Kosteli et al., 2010; Mottillo et al., 2010). This is observed even in chow-fed caveolin-1 null adipose tissue (Fig. 5F). Moreover, high fat diet feeding leads to a higher incidence of adipocyte death in caveolin-1 null mice as judged by the increased occurrence of perilipin negative adipocytes (Fig. 5G).

Mitochondrial function is challenging to assess directly in adipose tissue as the lipid-rich environment easily harms and/or uncouples the mitochondrial during isolation procedures. Therefore, we characterized the role of caveolin-1 in mitochondrial function *in vitro* using wildtype and caveolin-1 null mouse embryonic fibroblasts (MEFs). We found that wildtype MEFs were able to increase oxygen consumption in glucose-deprived media, while caveolin-1 null MEFs displayed a preference for glycolysis. To achieve that, we have altered the relative content of pyruvate and glucose in the incubation media and tested the degree of acidification of the supernatants and compared it to the rate of oxygen consumption (Fig. 6A). This finding is consistent with the initial *in vivo* observations of this study (e.g. increased RER during fasting and build-up of lactate upon PEPCK inhibition) that suggest an altered mitochondrial metabolism. In line with a recently published study (Bosch et al., 2011), we also found that caveolin-1 null MEF mitochondria display a dramatically higher membrane potential than wild type controls (Fig. 6B). We have previously shown that a modest overexpression of the mitochondrial dicarboxylate carrier (mDIC), an inner mitochondrial membrane carrier, results in hyperpolarization of mitochondria and increased oxidative damage (Das et al., 1999). Interestingly, caveolin-1 null MEFs have significantly higher mDIC mRNA expression compared to wildtype MEFs (Fig. 6C). Even though we do not know whether this increase in mitochondrial membrane potential is also present in caveolin-1 null adipocytes, we do see a significant 2-fold increase in the levels of the mDIC mRNA in adipose tissue, while the levels in liver are similar in wildtype and caveolin-1 null

mice (Fig. 6C). Similar observations were made at the protein level. The more marked mDIC expression difference in adipose tissue as compared to MEFs may depend on the stimulatory effect of FFAs on mDIC expression *in vivo* (Das et al., 1999). Thus, the local increase in FFAs contributes to the mitochondrial alterations in caveolin-1 null adipose tissue and is associated with increased ROS-mediated damage. These defects in turn cause the widespread increased occurrence of adipocyte death found in the adipose tissue of caveolin-1 null mice.

Mitochondria isolated in the context of *in vitro* experiments showed similar mitochondrial function in both liver and lung (a caveolin-1-rich tissue) from wild type and caveolin-1 null mice (Suppl. Fig 5A–B). Thus, even though caveolin-1 null MEFs display mitochondrial alterations, our data suggest that altered mitochondrial function is not a ubiquitous phenomenon in caveolin-1 null tissues. Alternatively, the alterations in mitochondrial function in caveolin-1 null cells could be secondary to defects of other cellular functions (e.g. lipid trafficking) and therefore are only apparent in the context of intact cells.

Elevated circulating BCAA levels in caveolin-1 null mice

Kahn and colleagues have recently shown that changes in the levels of BCAA catabolizing enzymes exclusively in adipose tissue have an impact on systemic levels of BCAAs (Herman et al., 2010). We found an increase in circulating levels of BCAAs in the caveolin-1 null mice (Fig. 6D). BCAAs are essential amino acids that are important for muscle growth by both stimulating anabolic pathways in general as well as serving as building blocks for muscle proteins (Blomstrand et al., 2006; Yamamoto et al., 2010). In fact, a recent study shows that administration of BCAA reverses dexamethasone-induced muscle atrophy (Yamamoto et al., 2010). Thus, the elevated circulating levels of BCAA may explain why lean body mass is preserved despite the increased rate of gluconeogenesis in the caveolin-1 null mice. BCAAs can stimulate muscle anabolism through the mTOR pathway involving the mTORC1 complex. Consistent with this mechanism, we found that phospho-mTOR levels were elevated in *m. gastrocnemius* in caveolin-1 null mice (Fig. 6E). The mTOR pathway can also up-regulate mitochondrial function, but over-activation of this pathway can lead to insulin resistance. Insulin resistant muscle cannot dispose of glucose as well and has to rely more on fatty acid oxidation to meet its energy requirements. The serum acylcarnitine profile in fasted state and the increased glucose levels in refed caveolin-1 null mice are both consistent with enhanced mitochondrial function and reduced insulin-induced glucose disposal in muscle. There are several possible mechanisms that could explain this difference in circulating BCAAs. These relate to the fact that caveolin-1 null mice have an increase in food intake, have a reduced fat mass and also show a transcriptional down-regulation of branched chain amino acids (BCAA) metabolizing enzymes in adipose tissue. To determine whether the transcriptional change was associated with a reduced catabolism and use of BCAAs in adipose tissue of the caveolin-1 null mice, we administrated tritium labeled leucine to fed and mildly fasted mice (Suppl. Fig. 6A and B). As expected, we found that the fed state is associated with a 10-fold increase in tritium counts in the organic phase, indicating that leucine is a significant lipogenic substrate in adipose tissue. To our surprise, the adipose tissues of the caveolin-1 null mice were taking up more leucine than wildtype adipose tissues, and this difference was more prominent in the lipid (organic) phase. In mildly fasted mice, the increase in tritium counts in adipose tissue of the caveolin-1 nulls was observed in all three phases, indicating an overall increase in leucine metabolism. Nevertheless, if the difference in body composition is taken into account, the overall tissue leucine uptake is similar between the wildtype and the caveolin-1 null mice. We conclude therefore that the transcriptional reduction of BCAA catabolizing enzymes in adipose tissue reflects a negative feedback rather than a functional defect of these enzymes and that the

increase in circulating BCAA levels is largely due to the increase in dietary intake in the caveolin-1 null mice.

Discussion

Systemic loss of caveolin-1 leads to a complex metabolic phenotype including a substantial decrease in metabolic inflexibility. This is also tightly associated with lower adiponectin levels and, in particular, lower levels of the HMW form of adiponectin. In fact, mice overexpressing adiponectin and mice lacking caveolin-1 display metabolic phenotypes at two opposite extremes of the spectrum of metabolic responses. At least part of this complex metabolic phenotype of the caveolin-1 null mouse is a compensatory response to severe metabolic dysregulation at the level of adipocytes. Importantly, reconstituting caveolin-1 expression in the endothelium in the context of a full body caveolin-1 null mouse did not restore the metabolic phenotype, but did improve cardiovascular and pulmonary hypertension phenomena, hence eliminating another likely cell type that could have contributed to a metabolic phenotype (Murata et al., 2007). Caveolin-1 null adipose tissue is insensitive to both insulin and adrenergic agonists likely due to the lack of caveolin-1, the key structural protein of caveolae in adipocytes that stabilizes the receptors and facilitates signaling (Liu et al., 2002). As judged by the enhanced response to the phosphodiesterase inhibitor enoximone, downstream signaling at the level of adrenergic agonists and glucagon appears to function properly, even in the absence of caveolin-1. Nevertheless, a high degree of metabolic inflexibility persists in the caveolin-1 null mouse. Our data suggest that this is not only due to a very complex set of changes that lead to the inability to accurately gauge the metabolic needs of the system, but is also caused by altered mitochondrial function.

Lack of caveolin-1 is associated with altered mitochondrial function at multiple levels. Caveolin-1 null MEFs display an increased dependence on glucose and a higher mitochondrial membrane potential. *In vivo*, we observe elevated circulating levels of H_2O_2 and an increased build-up of lactate upon PEPCK-inhibition in caveolin-1 null mice. In caveolin-1 null adipose tissue, we observe increased oxidative damage and an increased susceptibility to HFD-induced adipocyte death. Gene expression analysis also shows altered expression of many mitochondrial and redox-sensitive genes in adipose tissue, but not in the liver. At this point, we do not know whether the altered mitochondrial function is a consequence of the metabolic changes in the caveolin-1 null mice or if caveolin-1 deficiency directly has an impact on mitochondrial function. There are several potential mechanisms that can lead to the altered mitochondrial function observed in caveolin-1 null cells. One possibility is that the increased local levels of adipose tissue FFAs, driven by widespread elevated lipolysis in caveolin-1 null adipocytes, directly induce mitochondrial dysregulation and ROS production (a mechanism recently reviewed in (Vigouroux et al., 2011)). Several additional studies have highlighted that the rate of mitochondrial peroxide generation is significantly higher when basal respiration is driven by fatty acid oxidation compared to carbohydrate-based substrates (Anderson et al., 2007; St-Pierre et al., 2002). Previous studies from our laboratory show that FFAs can lead to an increase in mDIC, higher levels of which in turn elevate the mitochondrial potential (Das et al., 1999). In line with a cause / effect relationship, caveolin-1 null MEFs and adipose tissue display elevated mDIC levels. Increased membrane potential *per se* can be the cause for increased ROS production, leading to mitochondrial and metabolic dysfunction. Thus, the phenomenon of increased mitochondrial membrane potential may not necessarily directly depend on excess FFA levels in these cells. A second possibility is the mechanism suggested by Bosch and colleagues. They report an increase in mitochondrial cholesterol accumulation and a reduction in mitochondrial GSH in caveolin-1 deficient cells and suggest that this leads the mitochondrial impairments in these cells (Bosch et al., 2011). It is also possible that intracellular dysregulation of lipid species other than cholesterol plays a role for the

mitochondrial phenotype. Sphingolipids, such as ceramides, may show an altered subcellular distribution and play a role in this context. However, we mainly detect signs of mitochondrial alteration in adipose tissue, but not in other tissues where caveolin-1 is also expressed at high levels, such as the lung. This suggests that altered intracellular lipid partitioning alone cannot fully explain the mitochondrial alterations in caveolin-1 null mice. Hence, our present hypothesis that best explains our findings is that adipose tissue-resident cells are more vulnerable to mitochondrial changes induced by caveolin-1 deficiency through the elevated exposure of FFAs.

The elevated RER in caveolin-1 null mice suggests that the preference for glucose is not only an *in vitro* phenomenon, but also evident at the whole system level. Despite the increased use of glucose, the caveolin-1 null mice are not only able to maintain, but have, in fact, higher fasting glucose levels than the wildtype controls. This is due to a vastly increased capacity for hepatic glucose production. In particular, we observe an increased capacity to produce glucose from glycerol in the caveolin-1 null mice. However, the elevated levels of circulating urea also suggest that the glucose overproduced in the caveolin-1 null mouse is in part generated from an enhanced amino acid catabolism. In general, enhanced amino acid catabolism leads to muscle wasting. However, caveolin-1 null mice do not have reduced muscle mass. There may well be several mechanisms underlying this complex phenotype, but we chose to focus on secondary adaptations due to the severe defects observed in the adipose tissue (this study and (Cohen et al., 2004; Cohen et al., 2003; Razani et al., 2002). Our rationale to this approach was mainly that the liver-specific caveolin-1 null mice lack a substantial liver phenotype, and that the reported muscle phenotype of the caveolin-1 null mouse appears to be more pronounced as the mice age (Schubert et al., 2007).

From gene expression profile analysis of adipose tissue, we found that the pathway for BCAA catabolism is down-regulated. On the contrary, our leucine tracer studies showed that leucine is more effectively taken up and used in the lipogenic pathway in caveolin-1 null adipose tissue compared to wildtypes. Thus, the transcriptional reduction of BCAA metabolizing enzymes result from a negative feed-back mechanism and is not the cause of the higher circulating BCAA levels in the caveolin-1 null mice. Moreover, we confirm that excess dietary BCAAs feed into the lipogenic pathway in mature adipocytes (Frerman et al., 1983). BCAAs are not only an important metabolic building block and precursor, but have been shown to stimulate anabolic pathways through the mTOR-pathway. Furthermore, isoleucine prevents accumulation of triglycerides in liver and muscle through a mechanism that involves up-regulation of PPARα and UCPs, resulting in increased fatty acid oxidation (Nishimura et al., 2010). On the other hand, elevated BCAAs in diet-induced obesity have recently been shown to induce insulin resistance as a consequence of chronic activation of the mTOR pathway (Newgard et al., 2009). All these effects assigned to BCAAs fit very well with the phenotype of the caveolin-1 null mouse. The muscles of the caveolin-1 null mouse display enhanced mitochondrial proliferation (Schubert et al., 2007) and elevated levels of phospo-mTOR, and the brown adipose depot has elevated levels of UCP1 (Mattsson et al., 2010). However, we do not exclude that caveolin-1 may also play a direct role for insulin resistance and mitochondrial proliferation in the skeletal muscle in caveolin-1 null mice as also suggested by Oh, Schubert and colleagues (Oh et al., 2008; Schubert et al., 2007). The main findings of our study are summarized in Fig. 6F.

What is the relevance of the caveolin-1 null mouse for human biology and disease? There are a few reports on caveolin-1 deficiency, leading to lipodystrophy, but this condition is very rare (Garg and Agarwal, 2008). However, a relative decrease in caveolin-1 and “caveolar dysfunction” has been suggested to play a role in the metabolic syndrome (Fernandez-Real et al., 2010; Venugopal et al., 2004). Obese subjects have also been shown

to display elevated levels of BCAAs (Newgard et al., 2009). Moreover, several studies suggest that mitochondrial dysfunction in adipose tissue contributes to metabolic disturbances associated with obesity (De Pauw et al., 2009; Maassen, 2006). It may be that enhanced glucose production in insulin resistant states is further aggravated by factors and metabolic alterations originating from suboptimal mitochondrial function in adipose tissue. We do not yet fully understand the underlying mechanism for the lower adiponectin levels in the caveolin-1 null mice, but the altered mitochondrial function (leading to an altered energetic state of the adipocyte) and the increased levels of reactive oxygen species are likely contributing factors (Koh et al., 2007; Sun et al., 2009). In this study, we discovered a striking positive correlation in between pyruvate and adiponectin, which may be related to the antioxidant capacity of pyruvate. Further detailed studies are required to fully understand the regulation of adiponectin levels as well as the specific role of mitochondrial alterations in adipose tissue for systemic metabolic disease.

Many tumor cells lose caveolin-1 in the early phase of transformation, and caveolin-1 is well-known for its tumor suppressor activity through inhibition of several anabolic pathways (Williams and Lisanti, 2005). However, a high rate of proliferation requires enhanced aerobic glycolysis as opposed to oxidative phosporylation. Thus, altered mitochondrial function associated with loss of caveolin-1 may contribute to an increase in glycolysis and thereby enable proliferation. The overall metabolic environment of the full body caveolin-1 null knockout may therefore predispose cells to transformation. In fact, Lisanti and colleagues have proposed a model where loss of caveolin-1 in tumor-associated fibroblasts increases oxidative stress and causes increased tumor growth (Trimmer et al., 2011). We support that hypothesis and the full caveolin-1 null mouse indeed displays elevated circulating H_2O_2 levels. Moreover, tumor growth depends on high influx of nutrients such as glucose and BCAAs and is inhibited by pyruvate. This demand is met by an upregulation of various nutrient transporters, and a selective decrease in the Sodium-Coupled Monocarboxylate Transporter 1 (SMCT1) that primarily transports butyrate and pyruvate, which are inhibitors of histone deacetylases and thereby can induce tumor cell apoptosis (Ganapathy et al., 2009). Thus, the increased levels of BCAAs and glucose, and the reduced levels of pyruvate may also promote tumor progression in the caveolin-1 null mouse.

In summary, caveolin-1 null mice are lean and muscular, but show a decreased metabolic flexibility and an increased predisposition for malignant transformation, ultimately leading to a shorter life span (Park et al., 2003). Our data suggest that the complex phenotype of the caveolin-1 null mouse to a large extent depends on metabolic and mitochondrial alterations at the level of the adipocyte. The metabolic adaptations that occur in the caveolin-1 null mice may serve as a model for the effects of changes in mitochondrial function observed in obesity as well as in cancer metabolism.

Materials and Methods

Animals

Caveolin-1 null mice and liver-specific caveolin-1 null mice were used on the FVB background. The strategy for the generation of the liver-specific caveolin-1 null mice is shown in Supplemental Fig. 3B. All mice were backcrossed at least 10 times to their respective background. Mice were maintained on a 12 hour dark/light cycle and housed in groups of 2–4 in with unlimited access to water, chow (No. 5058, Lab-Diet) or high fat diet (HFD) (No. D12492, Research Diets Inc.) as indicated for the individual experiments. The Institutional Animal Care and Use Committee of the University of Texas Southwestern Medical Center, Dallas, has approved all animal experiments.

Adiponectin size fractionation

Analysis of the adiponectin complex distribution was performed as described in Schraw et al. (Schraw et al., 2008) and analyzed using a rabbit polyclonal anti-mouse adiponectin primary antibody (Scherer et al., 1995).

β3-AR-agonist sensitivity test

Tail vein serum samples were obtained before and 5, 15 and 60 minutes after an intraperitoneal injection of 1 mg/kg CL 316,243 (Sigma, Sigma Aldrich, USA).

Hepatic Steatosis measurements

Quantification of hepatic steatosis was performed by computerized tomography (CT) as previously described (Asterholm and Scherer, 2010). In brief, mice were anesthetized with isoflurane and a CT-scan was performed at a resolution of 93 μm using the short scan mode (180°) on a eXplore Locus *in vivo* MicroCT Scanner from GE Healthcare. Liver lipid content was estimated by obtaining the average CT-value in multiple regions well within the liver, as validated in (Asterholm and Scherer, 2010).

Liver histology—A subset of livers were fixed in methanol-free 4% paraformaldehyde for 20–24 hours, cryoprotected with sequential 10% and 18% sucrose equilibrations for 12-hours-each at 4°C, and then cryo-embedded in optimal cutting temperature medium (OCT, Sakura Finetek, USA). Multiple plane 8μm thickness cryostat sections were prepared of each liver and temporarily stored at −80°C. Staining for lipids with Oil Red-O was conducted according to established histologic protocol (Sheehan, 1980).

3-MPA treatment

3-Mercaptopicolinic Acid (3-MPA, Toronto Research Chemicals Inc.) was dissolved in PBS and 30 mg/kg was given orally at the indicated time-points.

Glycerol tolerance test

Thirty minutes after an oral dose of 30 mg/kg 3-MPA, the mice were injected i.p. with 1g/kg glycerol (0.1g/mL in PBS). Tail vein serum samples were obtained just prior and 15, 30, 60 and 120 minutes after the glycerol injection.

Metabolic response to phospodiesterase inhibitor

The mice were fasted for 5h prior i.p. injection with 10mg/kg enoximone (Sigma) dissolved in 2% Tween in PBS. Tail vein serum samples were obtained before and 30, 60, 120 and 180 minutes after the injection.

Blood and tissue biochemistry

Insulin and adiponectin levels were measured by commercial ELISA kits (Millipore, USA). Glucagon levels were measured in protease inhibitor treated blood samples with a Millipore RIA kit. Glucose and glycerol levels were determined with Sigma Diagnostics Glucose Reagents and Free Glycerol Reagent (Sigma, Sigma Aldrich, USA). Free fatty acid (FFAs) levels were measured with NEFA-HR(2) (Wako Pure Chemical Industries, Japan) and triglycerides with Infinity reagent (Thermo Scientific, USA). Urea was measured with a Vitros 250 Analyzer. Lactate, pyruvate, hydrogen peroxide, branched-chain amino acids (BCAAs) and glycogen were all measured by commercial kits (BioAssay Systems and Biovision). Local FFA levels in adipose tissue were measured by mincing approx. 50 mg freshly dissected gonadal adipose tissue. To break membranes, minced tissue samples were put in ice-cold hypotonic buffer (10mM TRIS-HCl, pH 7.5) and passed through a 22G

syringe. The homogenates were centrifuged (1000×g, 5min) at +4°C and FFAs were measured in the infranatant.

Metabolic and mitochondrial analysis of MEFs

For the experiments with wildtype and caveolin null MEFs, cells were isolated from 13.5 day embryos and maintained in low glucose DMEM plus 10% FCS. The day before the experiment, 40,000 cells were plated in XF24 V7 cell culture microplates. On the day of the experiment, the media was replaced with unbuffered XF assay media equilibrated for 1 hour and transferred to a temperature-controlled (37°C) Seahorse analyzer to measure the basal oxygen consumption rate. To measure the mitochondrial content and mitochondrial membrane potential cells were trypsinized and labeled 30 min at 37°C with mitotracker (200 nM) or tetramethylrhodamine methyl ester (TMRM-0.2μg/ml) in PBS. The cells were washed by centrifugation with PBS and analyzed in the FL2 channel of a FACSCalibur instrument.

^{3}H-Triolein uptake and oxidation

For tissue-specific lipid-uptake and lipid-oxidation analyses, ^{3}H-triolein was tail-vein injected into mice following a 5-h fast. After 15 min, tissues were harvested and lipids were extracted using a chloroform-to-methanol based extraction method. Samples were then counted for radioactivity.

Statistical Analysis

Data are in generally expressed as mean +/− standard error of the mean (SEM). The Student's t-test was used for comparisons between groups, log-transformation was performed as necessary to obtain normal distribution and a p-value <0.05 was considered as significant and is indicated by a single asterisk; double asterisk: $p<0.01$; triple asterisk: $p<0.001$.

Supplementary Material

Refer to Web version on PubMed Central for supplementary material.

Acknowledgments

We would like to thank Drs. David A. Yurek and Joseph Brozinik at Lilly Inc. for acyl-carnitine measurements and Thomas Person for help with data management. Supported by the National Institutes of Health (grants R01-DK55758, R01-CA112023, RC1 DK086629 and P01DK088761-01 to P.E.S.). R.W.G.A. was supported by the Cecil H. Green Distinguished Chair in Cellular and Molecular Biology and National Institutes of Health (grants HL 20948, GM 52016). I.W.A. was supported with a fellowship from the Throne-Holst Foundation, the Swedish Research Council (2006–3931) and from VINNOVA (Marie Curie Qualification).

References

Adams SH, Hoppel CL, Lok KH, Zhao L, Wong SW, Minkler PE, Hwang DH, Newman JW, Garvey WT. Plasma acylcarnitine profiles suggest incomplete long-chain fatty acid beta-oxidation and altered tricarboxylic acid cycle activity in type 2 diabetic African-American women. J Nutr. 2009; 139:1073–1081. [PubMed: 19369366]

Anderson EJ, Yamazaki H, Neufer PD. Induction of endogenous uncoupling protein 3 suppresses mitochondrial oxidant emission during fatty acid-supported respiration. The J Biol Chem. 2007; 282:31257–31266.

Asterholm IW, Halberg N, Scherer PE. Mouse Models of Lipodystrophy Key reagents for the understanding of the metabolic syndrome. Drug Discov Today Dis Models. 2007; 4:17–24. [PubMed: 18193096]

Asterholm IW, Scherer PE. Enhanced metabolic flexibility associated with elevated adiponectin levels. Am J Pathol. 2010; 176:1364–1376. [PubMed: 20093494]

Babich H, Liebling EJ, Burger RF, Zuckerbraun HL, Schuck AG. Choice of DMEM, formulated with or without pyruvate, plays an important role in assessing the in vitro cytotoxicity of oxidants and prooxidant nutraceuticals. In Vitro Cell Dev Biol Anim. 2009; 45:226–233. [PubMed: 19184251]

Blomstrand E, Eliasson J, Karlsson HK, Kohnke R. Branched-chain amino acids activate key enzymes in protein synthesis after physical exercise. J Nutr. 2006; 136:269S–273S. [PubMed: 16365096]

Bosch M, Mari M, Herms A, Fernandez A, Fajardo A, Kassan A, Giralt A, Colell A, Balgoma D, Barbero E, et al. Caveolin-1 deficiency causes cholesterol-dependent mitochondrial dysfunction and apoptotic susceptibility. Curr Biol. 2011; 21:681–686. [PubMed: 21497090]

Burgess SC, Hausler N, Merritt M, Jeffrey FM, Storey C, Milde A, Koshy S, Lindner J, Magnuson MA, Malloy CR, et al. Impaired tricarboxylic acid cycle activity in mouse livers lacking cytosolic phosphoenolpyruvate carboxykinase. J Biol Chem. 2004; 279:48941–48949. [PubMed: 15347677]

Carlin JI, Harris RC, Cederblad G, Constantin-Teodosiu D, Snow DH, Hultman E. Association between muscle acetyl-CoA and acetylcarnitine levels in the exercising horse. J Appl Physiol. 1990; 69:42–45. [PubMed: 2394661]

Cohen AW, Razani B, Schubert W, Williams TM, Wang XB, Iyengar P, Brasaemle DL, Scherer PE, Lisanti MP. Role of caveolin-1 in the modulation of lipolysis and lipid droplet formation. Diabetes. 2004; 53:1261–1270. [PubMed: 15111495]

Cohen AW, Razani B, Wang XB, Combs TP, Williams TM, Scherer PE, Lisanti MP. Caveolin-1-deficient mice show insulin resistance and defective insulin receptor protein expression in adipose tissue. Am J Physiol Cell Physiol. 2003; 285:C222–235. [PubMed: 12660144]

Combs TP, Pajvani UB, Berg AH, Lin Y, Jelicks LA, Laplante M, Nawrocki AR, Rajala MW, Parlow AF, Cheeseboro L, et al. A transgenic mouse with a deletion in the collagenous domain of adiponectin displays elevated circulating adiponectin and improved insulin sensitivity. Endocrinology. 2004; 145:367–383. [PubMed: 14576179]

Curtis JM, Grimsrud PA, Wright WS, Xu X, Foncea RE, Graham DW, Brestoff JR, Wiczer BM, Ilkayeva O, Cianflone K, et al. Downregulation of adipose glutathione S-transferase A4 leads to increased protein carbonylation, oxidative stress, and mitochondrial dysfunction. Diabetes. 2010; 59:1132–1142. [PubMed: 20150287]

Das K, Lewis RY, Combatsiaris TP, Lin Y, Shapiro L, Charron MJ, Scherer PE. Predominant expression of the mitochondrial dicarboxylate carrier in white adipose tissue. The Biochem J. 1999; 344(Pt 2):313–320.

De Pauw A, Tejerina S, Raes M, Keijer J, Arnould T. Mitochondrial (dys)function in adipocyte (de)differentiation and systemic metabolic alterations. Am J Pathol. 2009; 175:927–939. [PubMed: 19700756]

Drab M, Verkade P, Elger M, Kasper M, Lohn M, Lauterbach B, Menne J, Lindschau C, Mende F, Luft FC, et al. Loss of caveolae, vascular dysfunction, and pulmonary defects in caveolin-1 gene-disrupted mice. Science. 2001; 293:2449–2452. [PubMed: 11498544]

el-Maghrabi MR, Claus TH, Pilkis J, Pilkis SJ. Regulation of 6-phosphofructo-2-kinase activity by cyclic AMP-dependent phosphorylation. Proc Natl Acad Sci U S A. 1982; 79:315–319. [PubMed: 6281762]

Fan JY, Carpentier JL, van Obberghen E, Grunfeld C, Gorden P, Orci L. Morphological changes of the 3T3-L1 fibroblast plasma membrane upon differentiation to the adipocyte form. J Cell Sci. 1983; 61:219–230. [PubMed: 6885939]

Fernandez-Real JM, Catalan V, Moreno-Navarrete JM, Gomez-Ambrosi J, Ortega FJ, Rodriguez-Hermosa JI, Ricart W, Fruhbeck G. Study of caveolin-1 gene expression in whole adipose tissue and its subfractions and during differentiation of human adipocytes. Nutr Metab. 2010; 7:20.

Frerman FE, Sabran JL, Taylor JL, Grossberg SE. Leucine catabolism during the differentiation of 3T3-L1 cells. Expression of a mitochondrial enzyme system. J Biol Chem. 1983; 258:7087–7093. [PubMed: 6304077]

Frohnert BI, Sinaiko AR, Serrot FJ, Foncea RE, Moran A, Ikramuddin S, Choudry U, Bernlohr DA. Increased adipose protein carbonylation in human obesity. Obesity. 2011; 19:1735–1741. [PubMed: 21593812]

Ganapathy V, Thangaraju M, Prasad PD. Nutrient transporters in cancer: relevance to Warburg hypothesis and beyond. Pharmacol Ther. 2009; 121:29–40. [PubMed: 18992769]

Garg A, Agarwal AK. Caveolin-1: a new locus for human lipodystrophy. J Clin Endocrinol Metab. 2008; 93:1183–1185. [PubMed: 18390817]

Goodman MN. Effect of 3-mercaptopicolinic acid on gluconeogenesis and gluconeogenic metabolite concentrations in the isolated perfused rat liver. Biochem J. 1975; 150:137–139. [PubMed: 1201006]

Grimsrud PA, Xie H, Griffin TJ, Bernlohr DA. Oxidative stress and covalent modification of protein with bioactive aldehydes. J Biol Chem. 2008; 283:21837–21841. [PubMed: 18445586]

Grujic D, Susulic VS, Harper ME, Himms-Hagen J, Cunningham BA, Corkey BE, Lowell BB. Beta3-adrenergic receptors on white and brown adipocytes mediate beta3-selective agonist-induced effects on energy expenditure, insulin secretion, and food intake. A study using transgenic and gene knockout mice. J Biol Chem. 1997; 272:17686–17693. [PubMed: 9211919]

Herman MA, She P, Peroni OD, Lynch CJ, Kahn BB. Adipose tissue branched chain amino acid (BCAA) metabolism modulates circulating BCAA levels. J Biol Chem. 2010; 285:11348–11356. [PubMed: 20093359]

Jimenez M, Leger B, Canola K, Lehr L, Arboit P, Seydoux J, Russell AP, Giacobino JP, Muzzin P, Preitner F. Beta(1)/beta(2)/beta(3)-adrenoceptor knockout mice are obese and cold-sensitive but have normal lipolytic responses to fasting. FEBS Lett. 2002; 530:37–40. [PubMed: 12387862]

Koh EH, Park JY, Park HS, Jeon MJ, Ryu JW, Kim M, Kim SY, Kim MS, Kim SW, Park IS, et al. Essential role of mitochondrial function in adiponectin synthesis in adipocytes. Diabetes. 2007; 56:2973–2981. [PubMed: 17827403]

Kosteli A, Sugaru E, Haemmerle G, Martin JF, Lei J, Zechner R, Ferrante AW Jr. Weight loss and lipolysis promote a dynamic immune response in murine adipose tissue. J Clin Invest. 2010; 120:3466–3479. [PubMed: 20877011]

Liu P, Rudick M, Anderson RG. Multiple functions of caveolin-1. J Biol Chem. 2002; 277:41295–41298. [PubMed: 12189159]

Maassen JA. Mitochondrial dysfunction in adipocytes: the culprit in type 2 diabetes? Diabetologia. 2006; 49:619–620. [PubMed: 16491392]

Mattsson CL, Csikasz RI, Shabalina IG, Nedergaard J, Cannon B. Caveolin-1-ablated mice survive in cold by nonshivering thermogenesis despite desensitized adrenergic responsiveness. Am J Physiol Endocrinol Metab. 2010; 299:E374–383. [PubMed: 20530737]

Mottillo EP, Shen XJ, Granneman JG. beta3-adrenergic receptor induction of adipocyte inflammation requires lipolytic activation of stress kinases p38 and JNK. Biochim Biophys Acta. 2010; 1801:1048–1055. [PubMed: 20435159]

Murata T, Lin MI, Huang Y, Yu J, Bauer PM, Giordano FJ, Sessa WC. Reexpression of caveolin-1 in endothelium rescues the vascular, cardiac, and pulmonary defects in global caveolin-1 knockout mice. J Exp Med. 2007; 204:2373–2382. [PubMed: 17893196]

Newgard CB, An J, Bain JR, Muehlbauer MJ, Stevens RD, Lien LF, Haqq AM, Shah SH, Arlotto M, Slentz CA, et al. A branched-chain amino acid-related metabolic signature that differentiates obese and lean humans and contributes to insulin resistance. Cell Metab. 2009; 9:311–326. [PubMed: 19356713]

Nishimura J, Masaki T, Arakawa M, Seike M, Yoshimatsu H. Isoleucine prevents the accumulation of tissue triglycerides and upregulates the expression of PPARalpha and uncoupling protein in diet-induced obese mice. J Nutr. 2010; 140:496–500. [PubMed: 20089773]

Oh YS, Khil LY, Cho KA, Ryu SJ, Ha MK, Cheon GJ, Lee TS, Yoon JW, Jun HS, Park SC. A potential role for skeletal muscle caveolin-1 as an insulin sensitivity modulator in ageing-dependent non-obese type 2 diabetes: studies in a new mouse model. Diabetologia. 2008; 51:1025–1034. [PubMed: 18408913]

Oosterveer MH, Grefhorst A, van Dijk TH, Havinga R, Staels B, Kuipers F, Groen AK, Reijngoud DJ. Fenofibrate simultaneously induces hepatic fatty acid oxidation, synthesis, and elongation in mice. J Biol Chem. 2009; 284:34036–34044. [PubMed: 19801551]

Park DS, Cohen AW, Frank PG, Razani B, Lee H, Williams TM, Chandra M, Shirani J, De Souza AP, Tang B, et al. Caveolin-1 null (−/−) mice show dramatic reductions in life span. Biochemistry. 2003; 42:15124–15131. [PubMed: 14690422]

Razani B, Combs TP, Wang XB, Frank PG, Park DS, Russell RG, Li M, Tang B, Jelicks LA, Scherer PE, et al. Caveolin-1-deficient mice are lean, resistant to diet-induced obesity, and show hypertriglyceridemia with adipocyte abnormalities. J Biol Chem. 2002; 277:8635–8647. [PubMed: 11739396]

Scherer PE, Lisanti MP, Baldini G, Sargiacomo M, Mastick CC, Lodish HF. Induction of caveolin during adipogenesis and association of GLUT4 with caveolin-rich vesicles. J Cell Biol. 1994; 127:1233–1243. [PubMed: 7962086]

Scherer PE, Williams S, Fogliano M, Baldini G, Lodish HF. A novel serum protein similar to C1q, produced exclusively in adipocytes. J Biol Chem. 1995; 270:26746–26749. [PubMed: 7592907]

Schraw T, Wang ZV, Halberg N, Hawkins M, Scherer PE. Plasma adiponectin complexes have distinct biochemical characteristics. Endocrinology. 2008; 149:2270–2282. [PubMed: 18202126]

Schubert W, Sotgia F, Cohen AW, Capozza F, Bonuccelli G, Bruno C, Minetti C, Bonilla E, Dimauro S, Lisanti MP. Caveolin-1(−/−)- and caveolin-2(−/−)-deficient mice both display numerous skeletal muscle abnormalities, with tubular aggregate formation. Am J Pathol. 2007; 170:316–333. [PubMed: 17200204]

Sheehan, D.; Hrapchak, B., editors. Theory and practice of Histotechnology. 1980.

Sonnino S, Prinetti A. Sphingolipids and membrane environments for caveolin. FEBS Lett. 2009; 583:597–606. [PubMed: 19167383]

Sparks LM, Ukropcova B, Smith J, Pasarica M, Hymel D, Xie H, Bray GA, Miles JM, Smith SR. Relation of adipose tissue to metabolic flexibility. Diabetes Res Clin Pract. 2009; 83:32–43. [PubMed: 19038471]

St-Pierre J, Buckingham JA, Roebuck SJ, Brand MD. Topology of superoxide production from different sites in the mitochondrial electron transport chain. J Biol Chem. 2002; 277:44784–44790. [PubMed: 12237311]

Sun J, Xu Y, Dai Z, Sun Y. Intermittent high glucose stimulate MCP-l, IL-18, and PAI-1, but inhibit adiponectin expression and secretion in adipocytes dependent of ROS. Cell Biochem Biophys. 2009; 55:173–180. [PubMed: 19756411]

Trimmer C, Sotgia F, Whitaker-Menezes D, Balliet RM, Eaton G, Martinez-Outschoorn UE, Pavlides S, Howell A, Iozzo RV, Pestell RG, et al. Caveolin-1 and mitochondrial SOD2 (MnSOD) function as tumor suppressors in the stromal microenvironment: a new genetically tractable model for human cancer associated fibroblasts. Cancer Biol Ther. 2011; 11:383–394. [PubMed: 21150282]

Utter MF, Keech DB, Scrutton MC. A possible role for acetyl CoA in the control of gluconeogenesis. Adv Enzyme Regul. 1964; 2:49–68. [PubMed: 5863094]

Varady KA, Allister CA, Roohk DJ, Hellerstein MK. Improvements in body fat distribution and circulating adiponectin by alternate-day fasting versus calorie restriction. J Nutr Biochem. 2010; 21:188–95. [PubMed: 19195863]

Varady KA, Hellerstein MK. Alternate-day fasting and chronic disease prevention: a review of human and animal trials. Am J Clin Nutr. 2007; 86:7–13. [PubMed: 17616757]

Venugopal J, Hanashiro K, Yang ZZ, Nagamine Y. Identification and modulation of a caveolae-dependent signal pathway that regulates plasminogen activator inhibitor-1 in insulin-resistant adipocytes. Proc Natl Acad Sci U S A. 2004; 101:17120–17125. [PubMed: 15569940]

Vigouroux C, Caron-Debarle M, Le Dour C, Magre J, Capeau J. Molecular mechanisms of human lipodystrophies: from adipocyte lipid droplet to oxidative stress and lipotoxicity. Int J Biochem Cell Biol. 2011; 43:862–876. [PubMed: 21392585]

Williams TM, Lisanti MP. Caveolin-1 in oncogenic transformation, cancer, and metastasis. Am J Physiol Cell Physiol. 2005; 288:C494–506. [PubMed: 15692148]

Yamamoto D, Maki T, Herningtyas EH, Ikeshita N, Shibahara H, Sugiyama Y, Nakanishi S, Iida K, Iguchi G, Takahashi Y, et al. Branched-chain amino acids protect against dexamethasone-induced soleus muscle atrophy in rats. Muscle & Nerve. 2010; 41:819–827. [PubMed: 20169591]

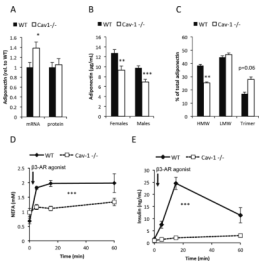

Figure 1. Caveolin-1 null mice display reduced circulating adiponectin levels and reduced sensitivity to β3-AR agonist

(A): mRNA and protein levels of adiponectin in 3 month old male mice (n=7–11 per group); **(B):** circulating levels of adiponectin in 2 month old mice (n=10–12 per group); **(C)**: adiponectin complex distribution in male mice match for total levels of adiponectin (n=3 per group). **(D)** and **(E)**: FFA and insulin response to β3-AR agonist (1mg/kg i.p.) in 2 months old male mice (n=4–5 per group). The error bars indicate SEM.

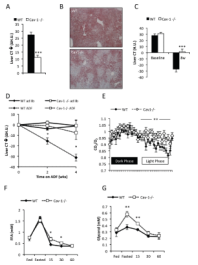

Figure 2. Reduced hepatic steatosis, reduced response to ADF, lower RER variability, but normal levels of fasting-induced FFAs the caveolin-1 null mice

Hepatic steatosis was assessed by CT measurements before and after a 24h fast (**A**) (note that the difference is plotted); **(B)** Representative ORO stain of livers from 24h fasted mice. Hepatic steatosis was assessed after 8 weeks of HFD feeding *ad libitum* (**C**) and followed by 4 weeks HFD feeding ADF or *ad libitum* HFD (**D**). Chow-fed mice were acclimatized to the metabolic cages for 4 days and on the 5th day RER (**E**) was recorded. Male mice 3–4 months old were used for panel A–E (n=4–10 per group). **(F–G)** show the levels of circulating FFAs and glycerol in the fed state at 7pm, 24h fasted state at 7pm and 15, 30 and 60 minutes after re-feeding (n=5 per group; 12 week old female cohorts used). The error bars indicate SEM.

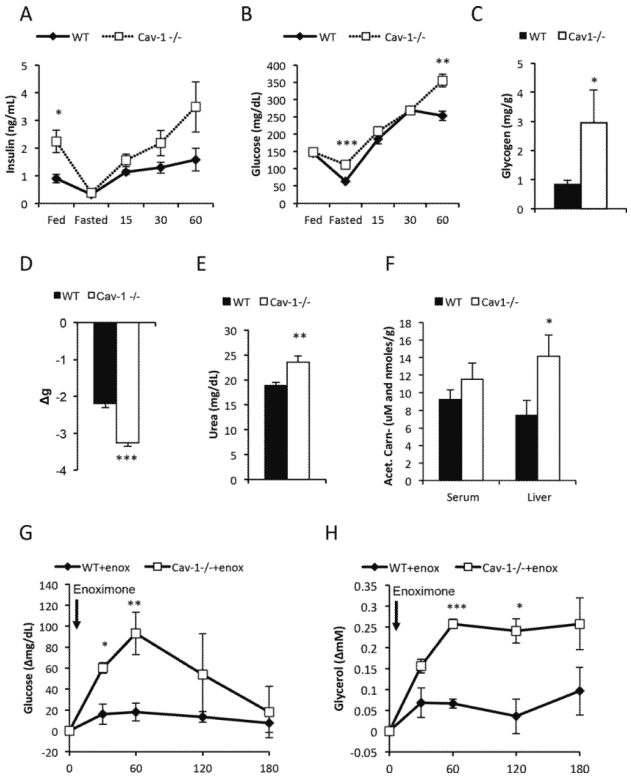

Figure 3. Caveolin-1 null mice have increased fasting glucose levels, increased breakdown of amino acids and an enhanced response to phospodiesterase inhibitor

(A–B)show the levels of circulating insulin and glucose in the fed state at 7pm, 24h fasted state at 7pm and 15, 30 and 60 minutes after re-feeding; (**C**) Glycogen levels in 5 hour fasted male mice (12 weeks old; n=5 per group); (**D**) Weight loss after 24h fasting. Circulating urea (**E**) and circulating as well as hepatic acetyl-carnitine levels (**F**) were measured in 5h male fasted mice (3 months old; n=7–9 per group). Enoximone (10 mg/kg i.p.) were injected to 5 hours fasted male mice (4 months old; n=3–5 per group) **(G–H)**: Enoximone-induced changes in glucose and glycerol levels. The error bars indicate SEM.

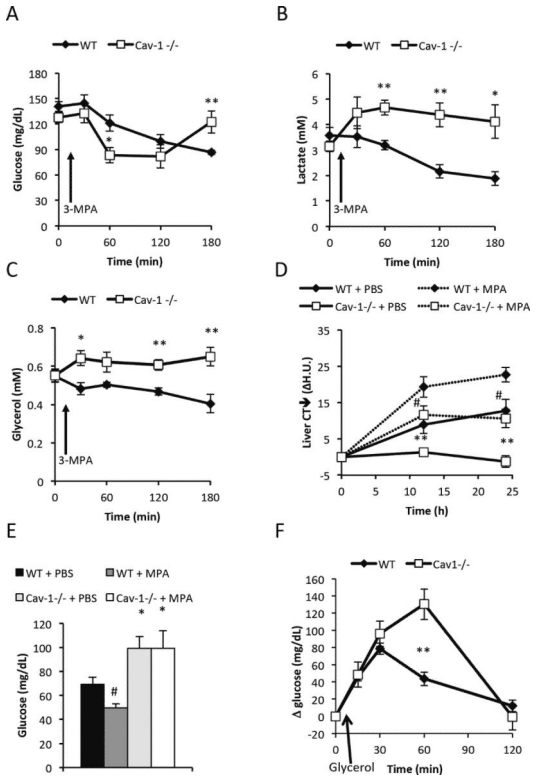

Figure 4. Caveolin-1 null mice display an altered response the PEPCK inhibition

Acute response to PEPCK inhibition: 12 week old female cohorts were fasted for 5h at daytime prior to intra-gastric administration of 30mg/kg 3-MPA (n=5 per group). Glucose levels were transiently lowered (**A**), while lactate (**B**) and glycerol (**C**) increased in the caveolin-1 null mice. Chronic response to PEPCK inhibition: Fasting-induced hepatic steatosis, followed by CT in female mice (8 month old; n=5 per group), was aggravated in presence of PEPCK inhibitor (**D**). Glucose levels were measured at the end of the time course and remained higher in both PBS and 3-MPA treated caveolin-1 null mice (**E**). (**F**) Glycerol-induced glucose production measured in PEPCK-inhibited female mice (3 months old; n=4–5 per group) was higher in caveolin-1 nulls indicating that the higher glucose levels in caveolin-1 null mice during fasting is mediated by an increase in glycerol-induced gluconeogenesis. The error bars indicate SEM.

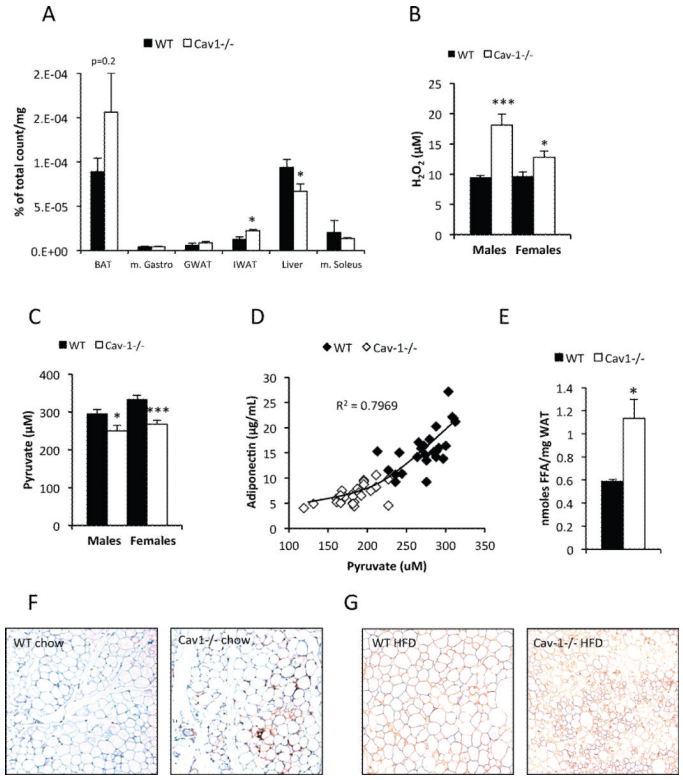

Figure 5. Caveolin-1 deficiency results in reduced hepatic triglyceride synthesis, increase in reactive oxygen species, elevated adipose tissue FFAs and increased macrophage infiltration

(**A**) Intravenous infusion of ^{3}H-triolein in mice fasted for 5h and reveals a reduced hepatic triglyceride synthesis in the liver of caveolin-1 null mice. Note that the ^{3}H count in the organic phase of adipose tissue (BAT and IWAT) was increased in the caveolin-1 null mice. This indicates an increase in triglyceride synthesis rate; (**B**) and (**C**): Circulating H_2O_2 and pyruvate levels in 2 month old mice after 5h of fasting (n=10−12 per group). (**D**) Adiponectin and pyruvate levels measured in female 4 month old mice were positively correlated. (**E**) Local FFA levels from gonadal adipose tissue pieces (n=4+4) obtained from 5 month old females. (**F**) and (**G**) Gonadal adipose tissue stained for respectively mac2 and perilipin. The error bars indicate SEM.

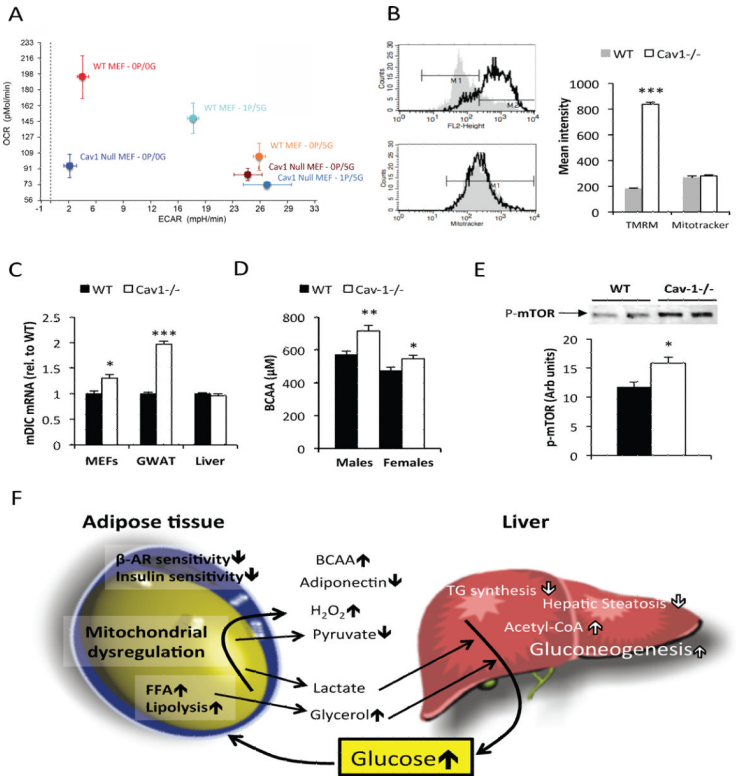

Figure 6. Altered mitochondrial function in Cav-1 null cells

(A) Caveolin-1 −/− MEFs display a preference for glycolysis. Cells were incubated in various concentrations (in mM) of pyruvate (P) and glucose (G) as indicated. Oxygen consumption rate (OCR) and extracellular acidification rate (ECAR) were measured in a Seahorse XF flux analyzer. **(B)** Caveolin-1 null cells have a higher mitochondrial membrane potential as judged by TMRM fluorescence intensity. **(C)** Comparison of wildtype and caveolin-1 null dicarboxylate carrier (mDIC) mRNA levels in MEFs, adipose tissue and liver. All measurements in MEFs reflect triplicate measurements. (**D**) BCAA levels after 5h of fasting in 2 month old mice (n=10−12 per group). (**E**) Phospho-mTOR levels were measured in *m. gastrocnemius* in 5h fasted, 3 month old male mice (n=6 per group). (**F**) Schematic representation of caveolin-1 null phenotype: Caveolin-1 deficiency leads to a reduced sensitivity to insulin and adrenergic agonists, elevated basal lipolysis, and is associated with altered mitochondrial function in adipose tissue. These defects have a profound impact on whole body metabolism. In the caveolin-1 null mice, we observe a dramatically enhanced hepatic glucose production as well as an increase in BCAA levels (likely due to increased food intake). We hypothesize that the elevated lipolysis and the altered mitochondrial function in adipose tissue (and possibly other tissues) exposes the liver to elevated levels of gluconeogenic substrates. The elevated BCAA levels both enhance fatty acid oxidation and increase anabolic processes in skeletal muscle. The error bars indicate SEM.

Table 1

Most profoundly affected canonical pathways

Canonical Pathway	p-value	Ratio
Adipose tissue		
Mitochondrial Dysfunction e.g. CO×8B ↓4.0, GPD2 ↓1.6	5.00E-10	59/172
Oxidative Phosphorylation e.g. ATP5A1 ↓1.7, ATP5F1 ↓1.6	6.86E-08	58/166
BCAA Degradation e.g ACAA2 ↓2.1, BCKDHA ↓1.3	3.62E-06	35/111
Liver		
Urea Cycle and Metabolism of Amino Groups e.g. ASL ↑1.7, CPS ↑1.5	7.51E-05	7/80
Mitochondrial Dysfunction e.g. CO×7A ↓1.1, NDUFA3 ↓1.3	3.61E-06	15/173
Oxidative Phosphorylation e.g. ATP 5E ↓1.2, ATP5F1 ↑1.3	1.82E-04	13/167

(Ratio: *Regulated genes/Total genes in pathway)*